

## RESEARCH ARTICLE

# Ppn2, a novel Zn<sup>2+</sup>-dependent polyphosphatase in the acidocalcisome-like yeast vacuole

Rūta Gerasimaitė and Andreas Mayer\*

**ABSTRACT**

Acidocalcisome-like organelles are found in all kingdoms of life. Many of their functions, such as the accumulation and storage of metal ions, nitrogen and phosphate, the activation of blood clotting and inflammation, depend on the controlled synthesis and turnover of polyphosphate (polyP), a polymer of inorganic phosphate linked by phosphoric anhydride bonds. The exploration of the role of acidocalcisomes in metabolism and physiology requires the manipulation of polyP turnover, yet the complete set of proteins responsible for this turnover is unknown. Here, we identify a novel type of polyphosphatase operating in the acidocalcisome-like vacuoles of the yeast *Saccharomyces cerevisiae*, which we called Ppn2. Ppn2 belongs to the PPP-superfamily of metallophosphatases, is activated by Zn<sup>2+</sup> ions and exclusively shows endopolyphosphatase activity. It is sorted to vacuoles via the multivesicular body pathway. Together with Ppn1, Ppn2 is responsible for a substantial fraction of polyphosphatase activity that is necessary to mobilize polyP stores, for example in response to phosphate scarcity. This finding opens the way to manipulating polyP metabolism more profoundly and deciphering its roles in phosphate and energy homeostasis, as well as in signaling.

**KEY WORDS:** Yeast vacuole, Inorganic polyphosphate, Polyphosphatase, Phosphate homeostasis

**INTRODUCTION**

Phosphorus is an essential macronutrient and a building block of nucleic acids, lipids and high-energy molecules. It is taken-up by cells in the form of inorganic phosphate (P<sub>i</sub>), the scarcity of which is often a limiting factor for growth of microorganisms and plants (Elser, 2012). Therefore, all organisms have developed elaborate systems of acquiring phosphate from the environment and complex regulatory mechanisms for adapting their metabolism in response to phosphate availability.

In all kingdoms of life, an integral part of phosphate metabolism is the synthesis of inorganic polyphosphate (polyP), a linear polymer ranging from several P<sub>i</sub> residues to thousands of P<sub>i</sub> residues in length (Kornberg et al., 1999). It is usually accumulated in acidic, Ca<sup>2+</sup>- and phosphate-rich membrane-enclosed compartments, called acidocalcisomes or acidocalcisome-related organelles (Docampo et al., 2005; Docampo and Huang, 2016). Substantial stores of polyP exist in prokaryotic and eukaryotic microorganisms. PolyP metabolism is tightly integrated into the overall energy

metabolism of the cell and polyP is used by the cells as a P<sub>i</sub> reserve and in phosphorylation and polyphosphorylation reactions (Azevedo et al., 2015; Livermore et al., 2016; Nocek et al., 2008; Rao et al., 2009). PolyP is important in detoxification of heavy metals and in counteracting alkaline and osmotic stress (Keasling, 1997; Pick and Weiss, 1991; Rohloff and Docampo, 2008). In addition, infectivity and persistence of prokaryotic and eukaryotic parasites depend on their polyP stores (Galizzi et al., 2013; Kim et al., 2002; Lander et al., 2013). The ability of polyP to stabilize proteins and act as a chaperone increases stress tolerance of cells (Azevedo et al., 2015; Dahl et al., 2015; Gray et al., 2014).

Mammalian cells contain much lower polyP levels compared to microorganisms (Kumble and Kornberg, 1995), but several important functions of mammalian polyP have been discovered. Upon activation, polyP is released from platelet-dense granules and modulates blood clotting and inflammation (Morrissey and Smith, 2015; Müller et al., 2009). PolyP can activate extracellular receptors (Dinarvand et al., 2014), modulate the excitability of neurons (Stotz et al., 2014) and protect cells from amyloid toxicity (Cremers et al., 2016). Although at times controversial (Faxalv et al., 2013), these findings have boosted interest in the polyP metabolism of eukaryotes. Further exploration of the role of acidocalcisomes and polyphosphates is hampered by our incomplete knowledge of the enzyme systems involved in polyP metabolism, even in the simple model organism *Saccharomyces cerevisiae*.

When phosphate is abundant in the medium, yeast accumulate large amounts of polyP, mainly inside the vacuole (Indge, 1968), an acidic, acidocalcisome-like organelle that degrades and recycles cellular compounds, accumulates and stores nutrients, and is tightly integrated into the signaling networks of the cell (Li and Kane, 2009). PolyP is used as a phosphate reserve that can sustain growth under phosphate scarcity or under acute high metabolic demand, as for example for dNTP synthesis during the S phase of the cell cycle (Bru et al., 2016). Synthesis and degradation of polyP are required to buffer cytosolic P<sub>i</sub> concentration, and this is essential for cells in order to adapt to changing phosphate availability in the environment. That cells actively regulate cytosolic P<sub>i</sub> is also underscored by the existence of a dedicated transcriptional program, the phosphate signal transduction (PHO) pathway (Thomas and O'Shea, 2005; Vardi et al., 2013), which responds to cytosolic P<sub>i</sub> levels. Since polyP metabolism does not only respond to cytosolic P<sub>i</sub> concentration but can even set it (Desfougères et al., 2016a), the exploration of polyP synthesis and turnover is crucial for understanding P<sub>i</sub> metabolism and nutrient signaling in general. This can only be achieved once the major proteins involved in polyP metabolism have been identified.

In yeast, polyP is synthesized from nucleoside triphosphates by the vacuolar transporter chaperone (VTC) complex, which localizes to the vacuole membrane and the cell periphery, likely the endoplasmic reticulum (Hothorn et al., 2009; Uttenweiler et al., 2007). Concomitantly with synthesis, VTC transfers a growing

Department of Biochemistry, University of Lausanne, Ch. des Boveresses 155, Epalinges 1066, Switzerland.

\*Author for correspondence (andreas.mayer@unil.ch)

 A.M., 0000-0001-6131-313X

Received 23 December 2016; Accepted 13 March 2017

polyP chain into the vacuole lumen (Gerasimaite et al., 2014). This process depends on the proton gradient across the vacuole membrane. Cells lacking VTC lose virtually all their polyP, suggesting that VTC is the major polyP polymerase in yeast (Desfougères et al., 2016a; Hothorn et al., 2009; Ogawa et al., 2000).

The situation with polyP degradation is more complex. Three proteins display polyphosphatase activities. Ppx1 is a highly processive exopolyphosphatase, degrading polyP by sequentially cleaving phosphate units from the end of a polyP chain (Wurst and Kornberg, 1994; Wurst et al., 1995). It is localized in the cytosol and therefore separated from the major polyP stores in the vacuole (Huh et al., 2003). Its deletion does not prevent degradation of polyP in response to low phosphate availability. It might, however, counteract the toxicity of cytosolic polyP (Gerasimaite et al., 2014). Ppn1 preferentially cleaves long polyP chains in the middle, but the end products of its reaction are triphosphate as well as monomeric  $P_i$  (Shi and Kornberg, 2005), suggesting that Ppn1 might also display exophosphatase activity. Ppn1 is localized inside the vacuole (Sethuraman et al., 2001). A third enzyme, Ddp1, has initially been described as diadenosine hexaphosphate and diphosphoinositol hydrolase. It has robust endopolyphosphatase activity *in vitro* (Cartwright and McLennan, 1999; Lonetti et al., 2011; Safrany et al., 1999). Similar to Ppx1, Ddp1 is localized in the cytosol and nucleus (Huh et al., 2003). Whereas the role of Ddp1 and its mammalian homologs in the metabolism of inositol pyrophosphates is well established, it is unclear whether its endopolyphosphatase activity is utilized *in vivo*.

A series of studies have detected polyphosphatase activities in different cellular compartments, such as the cell envelope, mitochondria, nucleus, cytosol and vacuoles (Lichko et al., 2006, 2003; Wurst et al., 1995). The enzymes responsible for these activities have been characterized by their cellular localization, molecular mass of the partially purified enzyme, the preferred metal ions and their differential sensitivity to inhibitors. However, the genes encoding these activities have never been identified, precluding studies of their *in vivo* roles. To our best knowledge, the only attempt to identify a gene by sequencing the N-terminus of a partially purified polyphosphatase led to the identification of the flavoprotein Yhb1, for which a role in polyP degradation has not been further explored (Lichko et al., 2000).

The difficulties in biochemically identifying missing polyphosphatase activities might be related to the fact that many phosphatases act on a wide spectrum of molecules *in vitro* – RNA, DNA, proteins and small molecules. This increases the chance that a promiscuous activity of unrelated enzymes towards polyP will be detected in extracts and mistaken for a genuine polyphosphatase activity (Mohamed and Hollfelder, 2013). In our efforts to identify missing *S. cerevisiae* polyphosphatases we chose a targeted approach based on data mining.

## RESULTS

As the vacuole stores most of the polyP in yeast, we scanned databases for promising candidates – vacuolar proteins of unknown function that contain motifs suggesting that they might hydrolyze phosphodiester or phosphoric anhydride bonds. We turned our attention to YNL217w, an uncharacterized open reading frame (ORF) coding for a 327-amino-acid (aa) protein with a weak similarity to metallophosphatases. High-throughput screens had suggested that the product of this gene might localize to the vacuole and interact with the vacuolar polyphosphatase Ppn1 (Breitkreutz et al., 2010; Huh et al., 2003). We term this protein Ppn2.

## Delivery of Ppn2 into the vacuolar lumen requires the MVB pathway

Ppn2 is a member of the phosphoprotein phosphatase (PPP) family, which is defined by three highly conserved sequence motifs (-GD<sub>X</sub>HG-, -GD<sub>X</sub>VDRG- and -GNHE-) that contain the catalytic residues. BLASTP searches in the non-redundant protein database did not reveal similarities of Ppn2 outside the ~100-amino-acid stretch containing these conserved motifs. The closest homolog of Ppn2 in the Protein Data Bank (PDB) is a symmetrically cleaving diadenosine tetraphosphate (Ap4A) hydrolase from *Shigella flexneri 2a* (Wang et al., 2006), which could be used to generate a homology model (Fig. 1A,B).

Ppn2 has a predicted transmembrane domain between residues 8 and 29, placing its putative catalytic domain at its C-terminus (Reynolds et al., 2008) (Fig. 1C). We investigated the localization of Ppn2 in the vacuole by genomically tagging it with yeGFP at the N- or C-terminus in the protease-deficient yeast strains BJ3505 and BY4742 *pep4Δ*. In order to test the topology of the protein, we subjected isolated vacuoles containing yeGFP–Ppn2 and Ppn2–yeGFP to limited proteolysis with proteinase K. yeGFP was readily cleaved from yeGFP–Ppn2, both in intact and detergent-solubilized vacuoles, indicating that the N-terminus faces the cytosol. In contrast, Ppn2–yeGFP could only be cleaved after solubilization of the vacuole membrane, indicating that the C-terminus of Ppn2 is localized in the lumen (Fig. 1D). Both constructs appear functional *in vivo* because they restore the typical polyP length distribution, which is lost in *ppn2Δ* cells (see below and Fig. 1E).

The fluorescence signals of the N- and C-terminally tagged proteins showed different patterns. While Ppn2–yeGFP stained exclusively the vacuole lumen, yeGFP–Ppn2 appeared on the vacuole membrane (Fig. 1F, left panel). Cleavage of yeGFP exposed to proteases in the vacuole lumen did not provide a satisfactory explanation for the luminal localization, because the constructs had been expressed in protease-deficient strains. Furthermore, the majority of Ppn2–yeGFP appeared as an intact fusion protein in western blots of vacuole extracts prepared from these cells (Fig. 1D, see lane ‘-’ for the Ppn2–yeGFP sample). Alternatively, one of the tags might interfere with sorting of Ppn2. Numerous hydrolases reach the vacuole via the multivesicular body (MVB) pathway, where they are first sorted into luminal vesicles of late endosomes, which then fuse with vacuoles and deliver these vesicles for degradation in the vacuole lumen (Hurley and Emr, 2006). Similar to the process for other hydrolases that are sorted via the MVB pathway, such as Ppn1 (Reggiori and Pelham, 2001) and Cps1 (Odorizzi et al., 1998), Ppn2 exposes only an 8-amino-acid N-terminal peptide to the cytosol. We propose that the attachment of a bulky GFP tag might render this peptide inaccessible for recognition by the ESCRT machinery and disturb sorting. We tested whether Ppn2 uses the MVB pathway by expressing Ppn2–yeGFP in a *vps4Δ* strain, in which sorting into luminal MVB vesicles is blocked (Babst et al., 1997). In this mutant, proteins using the MVB pathway remain in an enlarged MVB and on the vacuole membrane. We found Ppn2–yeGFP on the vacuole membrane of *vps4Δ* cells and in a large dot next to the vacuole, which is typical for the enlarged MVBs of a *vps4Δ* mutant (Fig. 1F, right panel). This suggests that Ppn2 reaches the vacuole lumen via the MVB pathway.

## Ppn2 is a Zn<sup>2+</sup>-dependent endopolyphosphatase

Our attempts to purify the hydrophilic domain of recombinant Ppn2 failed, as the protein remained insoluble. Therefore, we decided to investigate its activity using protein immunoprecipitated from yeast vacuoles. We overexpressed Ppn2 with an N-terminal 3HA tag in

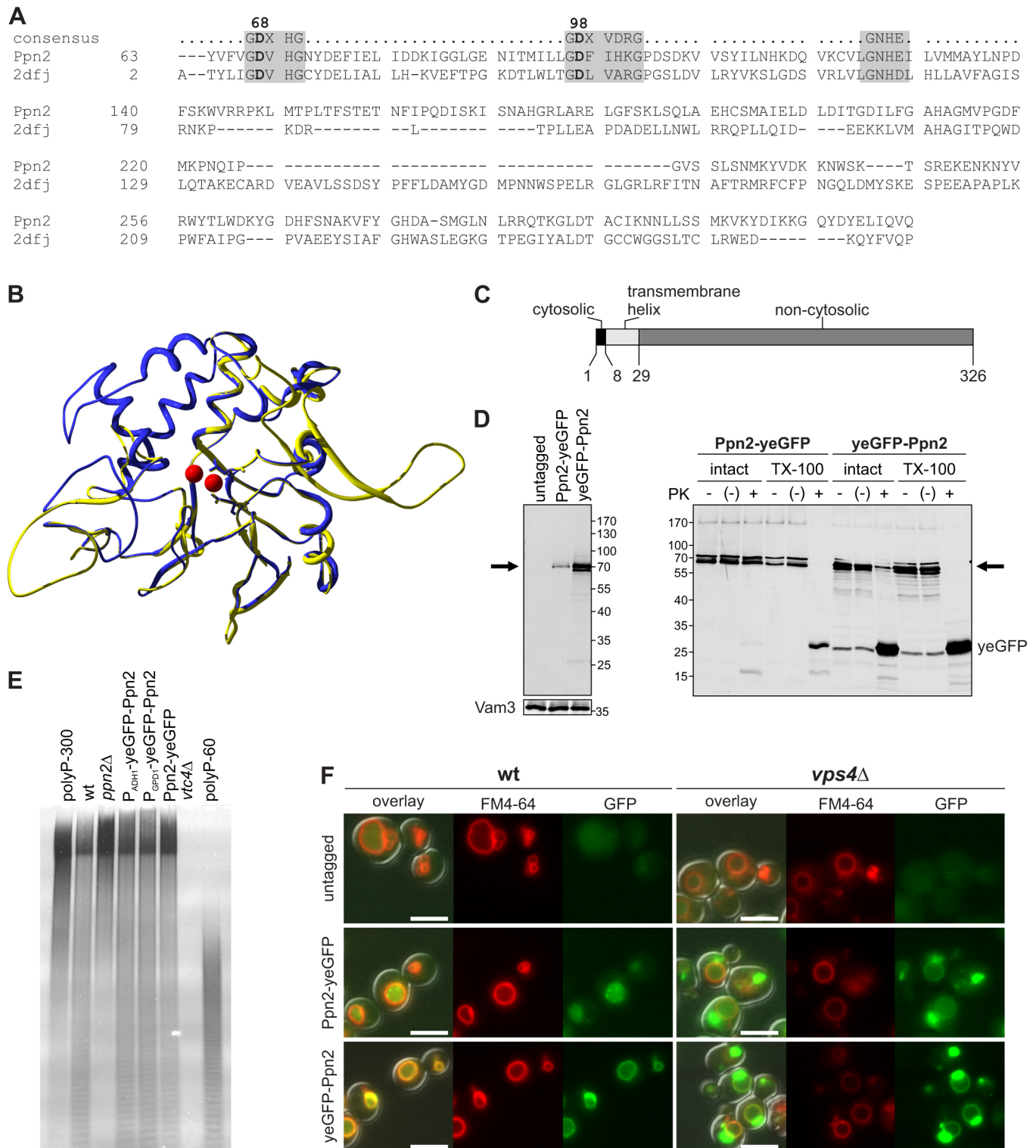


Fig. 1. See next page for legend.

yeast, using the strong  $GPD1$  promoter ( $P_{GPD1}$ -3HA-Ppn2). The protein was immunoprecipitated from vacuole detergent lysates with anti-HA antibody (Fig. 2A). When washed beads were incubated with synthetic polyP-60 (i.e. a 60-residue polyP chain) in the presence of  $ZnCl_2$ , a robust degradation activity was detected (Fig. 2B). No degradation was observed when vacuoles with non-tagged Ppn2 were used for immunoprecipitation.

High-throughput screens had suggested an interaction between Ppn2 and another vacuolar polyphosphatase, Ppn1. During our initial experiments, we found that the alkaline phosphatase Pho8 also co-immunoprecipitated with Ppn2 with high yield. Almost equal proportions of the total amount were co-precipitated for both proteins, suggesting that they form a stable complex. This is of interest because a recent report showed that Pho8 influences polyP

**Fig. 1. Structural features and cellular localization of Ppn2.** (A) Sequence alignment of Ppn2 and its closest homolog in the PDB database, diadenosine tetraphosphate (Ap4A) hydrolase from *Shigella flexneri* 2a (PDB code 2dfj). The conserved motifs of the PPP-superfamily are shaded, the aspartate residues critical for catalysis and metal ion chelation are in bold and their position in the Ppn2 sequence is indicated at the top. (B) Homology model of Ppn2 structure (yellow), produced using 2dfj as template (blue). The model was produced with SWISS-MODEL (Biasini et al., 2014). The critical aspartate residues highlighted in A are shown as sticks. Red spheres represent  $Mn^{2+}$  ions from the 2dfj structure. (C) Predicted topology of Ppn2. (D) Experimental determination of Ppn2 topology. Vacuoles were isolated from protease-deficient BJ3505 cells expressing Ppn2–yeGFP (endogenous promoter) or yeGFP–Ppn2 (ADH1 promoter). Left, western blot of isolated vacuoles to validate that anti-GFP antibody specifically recognizes tagged Ppn2; the vacuolar protein Vam3 is shown as a loading control. Right, the organelles were treated with proteinase K (PK) in the presence or absence of Triton X-100, precipitated with TCA and analyzed by SDS-PAGE and western blotting with anti-GFP antibody. PK treatments: +, PK added; –, no PK; (–), PK added after TCA. The arrow indicates GFP-tagged Ppn2. The position of molecular mass markers (in kDa) is also indicated. (E) yeGFP-tagged Ppn2 is functional *in vivo*. Wild-type (wt, BJ3505) or isogenic *ppn2Δ* cells, complemented by expression of Ppn2 fusion constructs as indicated, were logarithmically grown in YPD medium. PolyP was extracted, fractionated on 20% polyacrylamide gels and visualized by negative staining with DAPI. In this background, *ppn2Δ* loses short polyP chains even in the logarithmic phase, because the activation of Ppn2 is impaired by the absence of vacuolar proteases. The polyP chain length distribution of cells expressing Ppn2–yeGFP (endogenous promoter) and yeGFP–Ppn2 (ADH1 and GPD1 promoter) is similar to that of wt, indicating that Ppn2 is functional. (F) Localization of Ppn2 tagged with yeGFP on the N- (yeGFP–Ppn2, ADH1 promoter) and C-terminus (Ppn2–yeGFP, endogenous promoter) in BY4741 *pep4Δ* (left) and BY4741 *pep4Δ vps4Δ* (right) strains. Vacuole membranes were stained with FM4-64. The overlays include a Nomarski bright field image in order to show the cell boundaries. Scale bars: 5  $\mu$ m.

levels (Kizawa et al., 2016) and the homologous vacuolar alkaline phosphatase from *Candida utilis* has polyphosphatase activity (Fernandez et al., 1981). Therefore, we deleted *PPN1* and/or *PHO8* in  $P_{GPD1}$ -3HA-PPN2 cells and measured the activity of the immunoprecipitated 3HA–Ppn2. Immunoprecipitation efficiency of 3HA–Ppn2 was the same in all strains (Fig. 2A). Polyphosphatase activity was neither affected by *ppn1Δ* nor by a *pho8Δ* mutation, suggesting that Ppn2 carries a polyphosphatase activity that is independent of Ppn1 and Pho8 (Fig. 2B).

We identified conserved motifs of the PPP-family in Ppn2 and mutated Asp68 and Asp98 to Asn (Fig. 1A). These residues chelate the metal ion that is required for catalysis by lambda protein phosphatase (Zhuo et al., 1994). We expressed wild-type (wt) and mutant Ppn2 with an N-terminal 3HA tag from a centromeric plasmid. All proteins were expressed at similar levels, and could be immunoprecipitated with similar efficiency (Fig. 2C). As expected, 3HA–Ppn2<sup>wt</sup> showed robust degradation activity, while 3HA–Ppn2<sup>D68N</sup> and 3HA–Ppn2<sup>D98N</sup> were nearly inactive. Therefore, the conserved residues in the putative active center of Ppn2 likely play a similar role to those in other members of the PPP-superfamily. This result further supports the conclusion that Ppn2 is directly responsible for the observed polyphosphatase activity.

In order to examine the metal requirement of 3HA–Ppn2, we immunoprecipitated it in the presence of EDTA and measured its activity after re-addition of different divalent ions at 1 mM concentration (Fig. 2D). 3HA–Ppn2<sup>D68N</sup> remained inactive under all conditions. In contrast to other known yeast polyphosphatases, which can use  $Mg^{2+}$  for catalysis, 3HA–Ppn2<sup>wt</sup> remained inactive in the presence of  $Mg^{2+}$ . Only  $Zn^{2+}$  and  $Co^{2+}$  supported the catalytic activity of 3HA–Ppn2<sup>wt</sup>.  $Zn^{2+}$  is more likely to be used *in vivo* because it is stored to high levels inside vacuoles (Simm et al.,

2007).  $Co^{2+}$  has similar ionic radius and the same coordination geometry as  $Zn^{2+}$ , therefore it can effectively substitute for  $Zn^{2+}$ , and sometimes for other divalent metal ions, in the active sites of enzymes (Andreini et al., 2008). However, its concentration inside the cell is low and it is commonly accepted that only vitamin B<sub>12</sub>-dependent enzymes obligatorily require cobalt ions, where  $Co^{3+}$  serves as a redox center. More abundant divalent metal ions are more likely to be employed as Lewis acids in other enzyme classes.

### Ppn2 is an endopolyphosphatase

When we followed degradation of polyP-60 by 3HA–Ppn2<sup>wt</sup> by separating the reaction products on a gel, we noticed that shorter polyP chains accumulated before polyP disappeared entirely (Fig. 3A). This pattern is consistent with Ppn2 acting as a non-processive exopolyphosphatase or an endopolyphosphatase that cleaves inside the polyP chain. In order to test this more clearly, we measured the activity of 3HA–Ppn2<sup>wt</sup> by a Malachite Green assay that detects free  $P_i$  ions. Very low activity was detected, even with 8-fold higher protein concentration, compared to the preceding experiment where polyP-60 degradation had been followed by DAPI fluorescence (Fig. 3B). This residual activity disappeared completely when *PHO8* and *PPN1* were deleted, suggesting that Ppn2 by itself does not release  $P_i$ .

Next, we blocked the end groups of polyP-60 and polyP-300 by phosphoamidate linkage to spermidine (Choi et al., 2010) in order to render it resistant to exopolyphosphatase activity. This modified polyP could not be digested by purified recombinant *S. cerevisiae* yeast exopolyphosphatase (sc)Ppx1, serving as proof of successful modification (Fig. 3C). The modified polyP was still degraded by immunoprecipitated 3HA–Ppn2<sup>wt</sup>, but not by the catalytically inactive 3HA–Ppn2<sup>D68N</sup>. Thus, Ppn2 carries endopolyphosphatase activity.

### Ppn1 and Ppn2 account for a major share of the polyphosphatase activity of vacuole lysates

In order to determine whether, in addition to Ppn1 and Ppn2, vacuoles contain other major polyphosphatases, we sought to measure polyP hydrolysis activity in vacuoles from *ppn1Δ ppn2Δ* cells. However, our intense attempts to isolate vacuoles from this strain have failed. We had noticed previously that our vacuole isolation procedure yields vacuoles with low levels of polyP, even when the cells express hyperactive VTC and contain higher polyP levels than in wild type (Desfougères et al., 2016a). This is consistent with our observation that polyP is degraded during vacuole isolation (A.M., unpublished observation). We hypothesized that the failure to obtain vacuoles from *ppn1Δ ppn2Δ* might be caused by their inability to degrade polyP. In line with this assumption, the problem was overcome by deleting the catalytic subunit of the polyP polymerase (VTC4) in addition to the polyphosphatases. *vtc4Δ ppn1Δ ppn2Δ* cells gave good vacuole yields and allowed us to proceed with the experiments.

We compared the degradation of polyP-300 by detergent lysates of vacuoles from *vtc4Δ*, *vtc4Δ ppn1Δ*, *vtc4Δ ppn2Δ* and *vtc4Δ ppn1Δ ppn2Δ* strains (Fig. 4). In the presence of  $Mg^{2+}$ , the major polyphosphatase activity in vacuole lysates stemmed from Ppn1, as no activity was detected in vacuole extracts of *ppn1Δ vtc4Δ* and *ppn1Δ ppn2Δ vtc4Δ* strains. In the presence of  $Zn^{2+}$  ions, *ppn1Δ vtc4Δ* and *ppn2Δ vtc4Δ* both showed slower degradation than in wild type. This activity was completely absent in the *ppn1Δ ppn2Δ vtc4Δ* strain. Our assays yielded no evidence for vacuole-associated polyphosphatase activities other than Ppn1 and Ppn2, but they do not exclude that such activities exist and become significant under

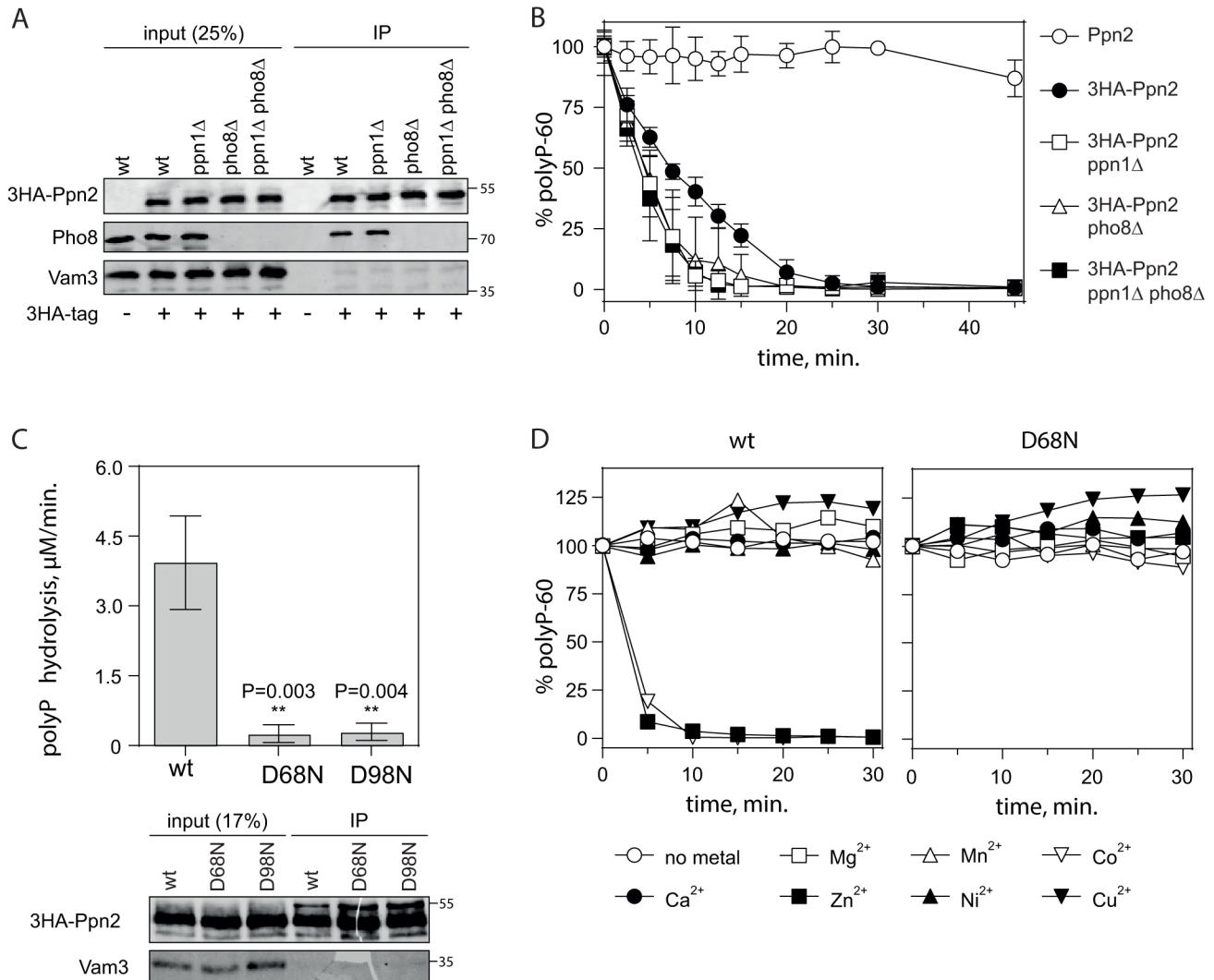


**Fig. 2. Polyphosphatase activity of immunoprecipitated 3HA-Ppn2.** (A) Immunoprecipitation (IP) of 3HA-tagged Ppn2 (3HA-Ppn2) by anti-HA antibody. 3HA-Ppn2 was expressed in BY4742 (wt) cells from genomically integrated constructs under the control of the GPD1 promoter (Table S1). Vacuoles were isolated, solubilized in Triton X-100 and pulled down with anti-HA antibodies. Adsorbed proteins were analyzed by SDS-PAGE and western blotting against the indicated proteins. The position of molecular mass markers (in kDa) is shown on the right. The vacuolar protein Vam3 is used as a loading control. (B) Degradation of polyP-60 by immunoprecipitated 3HA-Ppn2 from A. The reactions were performed in the presence of 1 mM ZnCl<sub>2</sub>. At the indicated time points, the remaining polyP-60 was quantified by measuring DAPI fluorescence. The experiment has been repeated with three independent vacuole preparations. Results are mean ± s.d. (C) Effect of substitution of the conserved aspartate residues in Ppn2. Wild-type and mutant proteins were expressed from the centromeric plasmid pRS415 under the control of the GPD1 promoter, immunoprecipitated from isolated vacuoles and assayed for polyP degradation as in B. Activities represent the mean ± s.d. of three independent vacuole preparations. \*\**P* < 0.05 (unpaired *t*-test). (D) Zn<sup>2+</sup> dependence of wt and mutant Ppn2. 3HA-Ppn2 (wt) and 3HA-Ppn2 (D68N) were immunoprecipitated in the presence of 1 mM EDTA, and the activity assays were performed with 1 mM of the chloride salts of the indicated metals. A representative result from two independent experiments is shown.

different experimental conditions. These results do, however, suggest that both Ppn1 and Ppn2 make major contributions to vacuolar polyP degradation.

#### Vacuolar polyphosphatases limit chain length but not the amount of polyP *in vivo*

In order to test for a role of Ppn2 in polyP metabolism *in vivo*, we quantified polyP levels in *ppn1Δ*, *ppn2Δ* and *ppn1Δ ppn2Δ* cells in the lag phase, logarithmic and stationary phase. Deletion of vacuolar polyphosphatases did not lead to increased polyP accumulation *in vivo* (Fig. 5A). In addition, vacuolar structure, which depends on the accumulation of polyP (Desfougères et al., 2016a), was not altered in the deletion mutants (Fig. 5C). By contrast, the average chain length showed strong changes (Fig. 5B).

In logarithmically growing BY4742 wild-type yeast, polyP chain length ranges from 3 to >300 P<sub>i</sub> residues. *ppn1Δ ppn2Δ* cells contained only chains longer than 300 units in all growth phases. As previously reported (Sethuraman et al., 2001), *ppn1Δ* cells contained longer polyP chains in the stationary phase. During the lag phase and logarithmic phase, however, polyP chain length distribution in *ppn1Δ* cells was similar to that in wild type. The effect of Ppn2 was the strongest during early logarithmic phase, when *ppn2Δ* cells showed a clear shift towards longer chains. Taken together with previous observations (Desfougères et al., 2016b), which suggested that the amount of polyP may be sensed inside the vacuole, our results suggest that polyP accumulation is mostly controlled by regulating the rate of the synthesis rather than degradation. In line with this, deletion of additional genes, such as

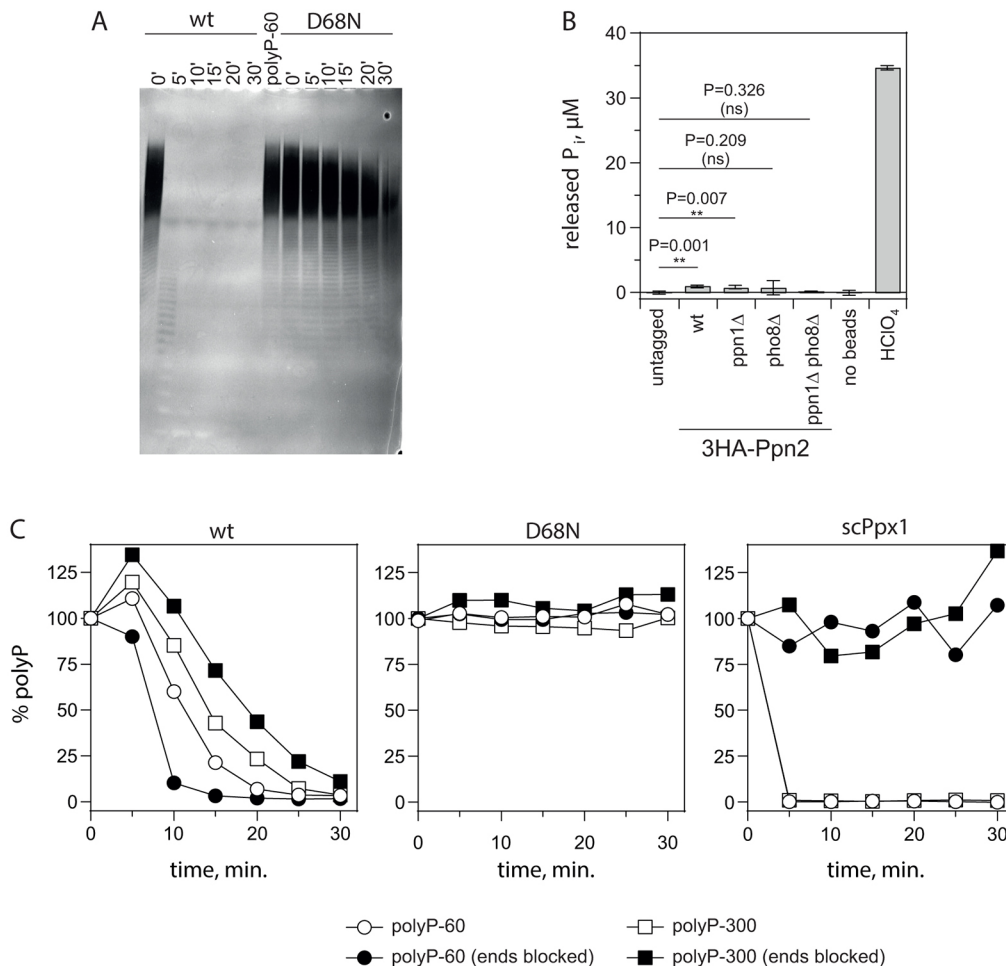


**Fig. 3. Ppn2 is an endopolyphosphatase.** (A) Degradation of polyP-60 by immunoprecipitated wild-type (wt) and D68N 3HA–Ppn2, monitored by gel electrophoresis. The reaction was stopped at the indicated time-points by mixing with phenol/chloroform and placing the samples on ice. PolyP was recovered by extraction with chloroform and ethanol precipitation. (B) Monitoring  $P_i$  release by immunoprecipitated 3HA–Ppn2 as in Fig. 2B by using the Malachite Green assay for free  $P_i$ . Note that in this experiment, 30  $\mu\text{M}$  polyP-60 was incubated (27°C, 30 min) with an 8-fold higher amount of immunoprecipitated 3HA–Ppn2 than in Fig. 2B. As a control, an equivalent amount of polyP-60 was totally hydrolyzed in 1 M HClO<sub>4</sub> at 99°C for 30 min and the released  $P_i$  was measured. The experiment was repeated with three independent vacuole preparations, error bars show mean $\pm$ s.d. \*\* $P$ <0.05; ns, not significant (unpaired  $t$ -test). (C) Degradation of polyP-60 and polyP-300 with chemically modified end groups. Immunoprecipitated 3HA–Ppn2 (wt) or 3HA–Ppn2 (D68N), and recombinant scPpx1 were used in polyP degradation assays run either with unmodified polyP, or with polyP that had its ends blocked by phosphoamidate linkage to spermidine. At the indicated time points, aliquots were assayed for polyP by DAPI fluorescence. A representative result from two independent experiments with independent vacuole preparations and two batches of chemically modified polyP-60 and polyP-300 is shown.

*PHO8* and *PPX1*, also did not increase cellular polyP levels in logarithmically growing cells (Fig. S1). Our results show that Ppn1 and Ppn2 make distinct contributions to vacuolar polyphosphate turnover in different growth phases. Furthermore, they suggest that the VTC complex is a highly processive enzyme that synthesizes very long chain polyP, and that the wide variation in chain lengths observed in wild-type cells results from polyP degradation by Ppn1 and Ppn2.

#### Ppn1 and Ppn2 are the major polyphosphatases required for polyP degradation in response to low $P_i$ availability

We next examined the effects of vacuole polyphosphatase knockouts on cell growth. No differences were detected in synthetic complete (SC) medium, when the cultures were started from logarithmically growing precultures (Fig. 6A). However, in SC medium with low levels of phosphate (SC- $P_i$ ), *ppn1* $\Delta$  *ppn2* $\Delta$  cells reduced their growth rate earlier and reached a lower final density than did wild-type cells. The same phenotype was observed with

*vtc4* $\Delta$  cells, which do not produce polyP. Loss of only one of the two vacuolar polyphosphatases did not produce a growth phenotype, suggesting that under these conditions Ppn1 and Ppn2 function redundantly.

Absence of polyphosphatase activity in vacuole extracts from double-knockout cells had suggested that Ppn1 and Ppn2 might be the most important vacuole polyphosphatases. In order to study their contribution *in vivo*, we assayed polyP mobilization after transferring the cells from  $P_i$ -rich medium to SC- $P_i$ . Transfer to low- $P_i$  medium induces rapid polyP degradation (Harold, 1966). Wild-type cultures fully degraded polyP within 2 h in SC- $P_i$  medium. *ppn1* $\Delta$  cultures showed a considerable delay and degraded their polyP only after 4–6 h. *ppn2* $\Delta$  cultures showed similar degradation kinetics to that of wild-type cells. *ppn1* $\Delta$  *ppn2* $\Delta$  cultures maintained their polyP stores throughout the incubation (Fig. 6B). We analyzed the chain length distribution during  $P_i$  limitation by gel electrophoresis (Fig. 6C).  $P_i$  limitation in wild-type cells was accompanied by a shift in polyP towards shorter chain lengths, followed by its complete

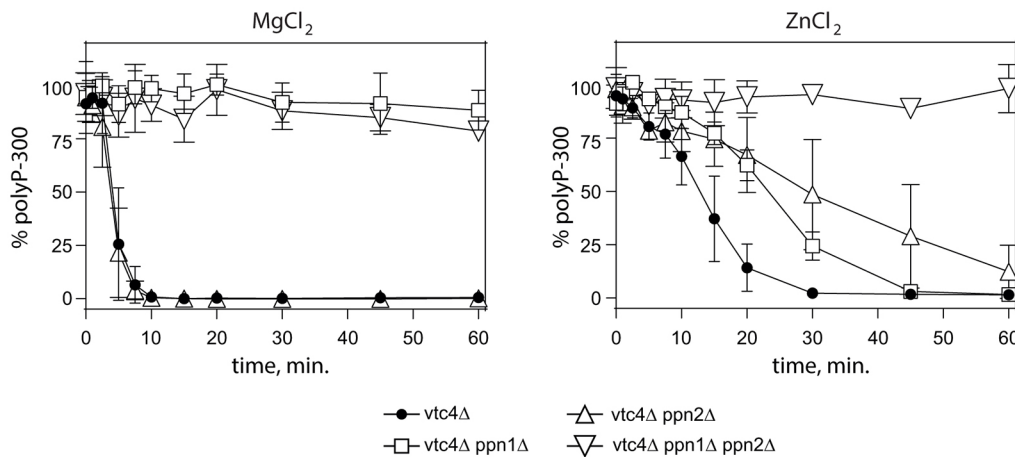


**Fig. 4. Contribution of Ppn1 and Ppn2 to total polyphosphatase activity of vacuole lysates.** Vacuoles were isolated from the indicated strains, solubilized in Triton X-100 and incubated with polyP-300 as a substrate, the remaining polyP-300 was then quantified at the indicated time points. The degradation assays were performed in the presence of 1 mM ZnCl<sub>2</sub> or 1 mM MgCl<sub>2</sub>. The experiment was repeated with three independent vacuole preparations, error bars show mean±s.d.

disappearance after 2 h of incubation. Whereas *ppn2Δ* had little effect, polyP degradation was delayed in *ppn1Δ* cells, with shorter polyP chains prevailing at the later time-points. PolyP in *ppn1Δ ppn2Δ* cells was, however, not converted into short chains, even after 6 h in low-P<sub>i</sub> medium. Taken together, these observations show that Ppn1 and Ppn2 have a major role in physiologically triggered polyP mobilization that is relevant for growth.

## DISCUSSION

*S. cerevisiae* has a complex system of polyP-degrading enzymes. Two polyphosphatases – Ppx1 and Ppn1 – were identified two decades ago, but it has soon been discovered that the deletion of both abolishes neither the *in vivo* mobilization polyP in response to P<sub>i</sub> scarcity nor polyP degradation by cell extracts *in vitro* (Lichko et al., 2006, 2008), but only slow these processes down. The contribution of the third yeast enzyme with polyphosphatase activity, Ddp1, was addressed by studying strains overexpressing Ddp1, which did not provide a clear answer concerning its *in vivo* relevance for polyP degradation (Trilisenko et al., 2015). The situation for Ddp1 is complicated by its role in metabolism of inositol pyrophosphates, which are crucial stimulators of polyP synthesis (Cartwright and McLennan, 1999; Safrany et al., 1999; Wild et al., 2016). Furthermore, its cytosolic and nuclear localization make it an unlikely candidate for degradation of the major vacuolar polyP stores. An earlier study had found two polyphosphatase activities associated with the vacuole (Wurst et al., 1995). While one of them was likely Ppn1 (Shi and Kornberg, 2005), the other one has remained unidentified. In this work, we show that a previously uncharacterized ORF, YNL217w, encodes the novel vacuolar polyphosphatase Ppn2, which, together with Ppn1, plays a major role in yeast polyP metabolism.

Why do the cells use two vacuolar enzymes for polyP degradation? Ppn1 and Ppn2 both have endopolyphosphatase activities and are sorted to the vacuole via the MVB pathway, but their sequences are unrelated. Having two unrelated enzymes with a similar function provides a means to differentially regulate polyP degradation in response to different stimuli or metabolic demands. The change of Ppn1 activity during culture growth has been noted previously (Shi and Kornberg, 2005). In line with this study, we observed that Ppn1 is important for defining polyP chain length in the stationary phase, whereas Ppn2 is most important at the beginning of logarithmic phase.

Ppn1 and Ppn2 seem to also have different biochemical properties. While Ppn1 was initially described as an endopolyphosphatase,

subsequent studies have shown that it could release P<sub>i</sub> (Andreeva et al., 2015; Sethuraman et al., 2001; Shi and Kornberg, 2005). Our data suggests that Ppn2 is exclusively an endopolyphosphatase and is unable to release P<sub>i</sub>. Although this result could be a consequence of the particular *in vitro* reaction conditions and should be interpreted with some caution, it might point to an important difference between Ppn1 and Ppn2. Ppn1 might be responsible for mobilization of polyP stores in response to increased demand for P<sub>i</sub>, while Ppn2 might control polyP chain length.

An earlier study found that polyP of 3 and 4 P<sub>i</sub> residues is generated from longer chains (Lusby and McLaughlin, 1980). We extend this observation and demonstrate *in vivo* that the VTC complex produces polyP chains longer than 300 P<sub>i</sub> residues. The typical broad distribution of polyP chain lengths, as seen in wild-type cells, should be ascribed to vacuolar polyphosphatases acting on these very long chains. It remains to be determined what advantage is provided to the cell by the ability to control the polyP chain length. It has been proposed that the accumulation of very long chains, or the lack of short chains of polyP, is toxic for yeast (Sethuraman et al., 2001). We were unable to reproduce this finding in our *ppn1Δ* and *ppn1Δ ppn2Δ* cells, perhaps because we used a different strain background. However, important physicochemical properties of polyP are defined by its length that might be of biological importance. First, the end and middle groups of polyP have different pK<sub>a</sub> values. While the middle groups are strongly acidic, the pK<sub>a1</sub> of the end groups is between 6.5 and 7.2 – close enough to the luminal pH of vacuoles to influence the buffering capacity of the vacuole lumen (Lee and Whitesides, 2010). Shifting the average chain length towards shorter chains can increase the concentration of the end groups and might play a role in controlling vacuolar and cytosolic pH. In line with this, degradation of longer polyP chains to triphosphate has been implicated in counteracting alkaline stress in the alga *Dunaliella salina*, and polyP degradation is observed during alkaline stress in *Trypanosoma cruzi* (Pick and Weiss, 1991; Ruiz et al., 2001). Second, at acidic pH (pH 5–6), longer polyP chains are better chelators of divalent metal ions than very short chains (polyP-3 or polyP-4). This can influence the ability of vacuoles to retain metal ions. Third, depending on ionic strength, pH and the presence of divalent metal ions, polyP chains readily form gels that can induce phase separations and provide separate reaction spaces (Cini and Ball, 2014). Finally, the ability of polyP to interact with proteins can depend on its chain length. This is illustrated by the observations that long polyP chains are more effective chaperones in bacteria (Gray et al., 2014), and that

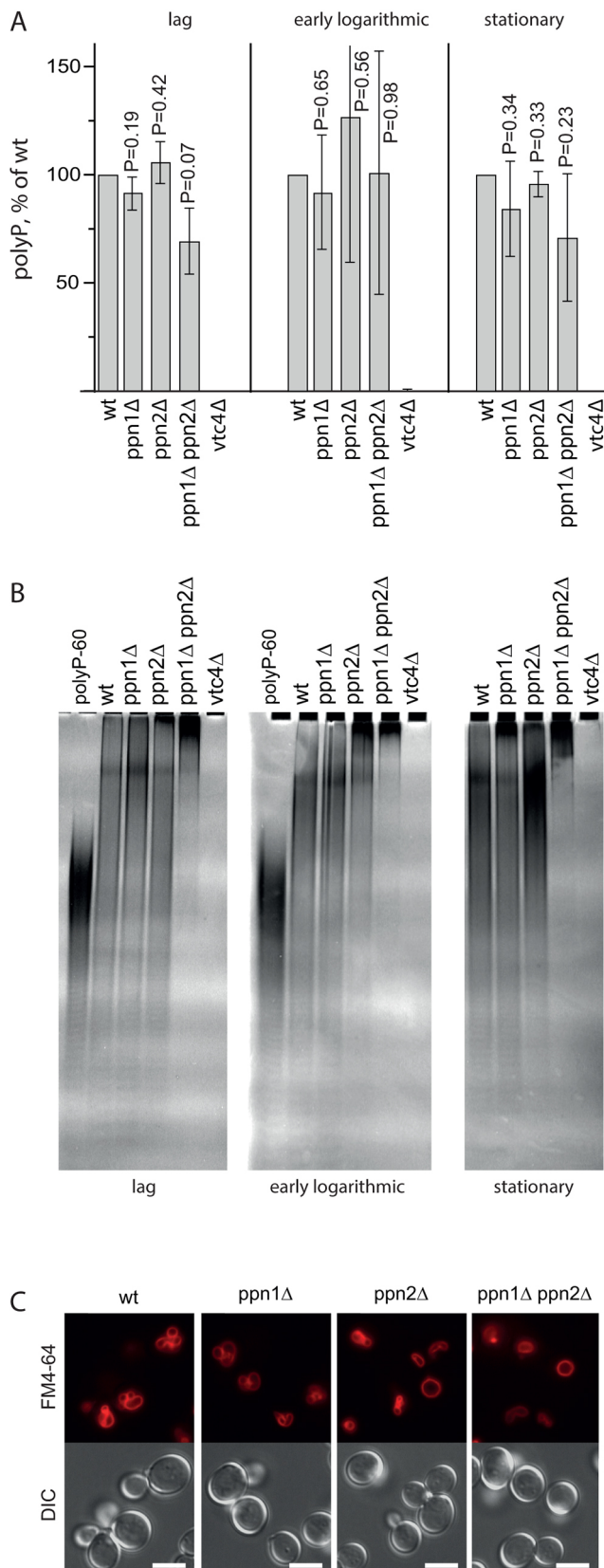


**Fig. 5. Effects of polyphosphatase knockouts on polyP accumulation, vacuole morphology and chain length *in vivo*.** (A) Poly P accumulation. The indicated strains were grown in SC medium as described in the Materials and Methods section. In the indicated growth phase, polyP was isolated by phenol/chloroform extraction with glass beads and, following degradation by scPpx1, quantified with a Malachite Green assay. PolyP content of the mutants was normalized to that of wild type (wt) in the corresponding growth phase. Differences in polyP content of the mutant strains are not significantly different from wt according to a one sample *t*-test (*P*-values are indicated). The experiment was repeated three times; results are mean±s.d. (B) For determination of polyP chain length, an amount equivalent to 2 μg of co-isolated RNA was withdrawn from the samples in A, treated with RNase A and proteinase K and fractionated on 25% polyacrylamide gels. PolyP was visualized by negative staining with DAPI. (C) Vacuole morphology of polyphosphatase knockout strains. The cells were grown in YPD to logarithmic phase (OD<sub>600</sub> of 1–2) and vacuole membranes were stained with FM4-64. A representative result from two independent experiments is shown. Scale bars: 5 μm.

If the physiological function of Ppn1 were to release P<sub>i</sub>, Ppn2 could accelerate this reaction by increasing the concentration of free polyP ends (substrates of exopolyphosphatase activity) and by decreasing the concentration of the competing long chains that are the preferred substrates for the endopolyphosphatase activity of Ppn1. Under the growth conditions that we have employed, we have not obtained compelling evidence for this mechanism, as *ppn2Δ* cells did not show a significant delay in polyP degradation in low-P<sub>i</sub> medium. However, our *in vitro* observations still argue for such a role: polyphosphatase defects in the vacuole lysates of *ppn1Δ* and *ppn2Δ* strains (as shown in Fig. 4) could only be detected when polyP-300 was used as a substrate. With shorter polyP-60 the differences were less pronounced and poorly reproducible. It is possible that the polyP degradation assays that we performed in SC-P<sub>i</sub> medium under standard laboratory conditions were not competent to reveal a similar effect *in vivo*.

The major polyP store of the yeast cell is inside the vacuole. Surprisingly, deletion of both the vacuole polyphosphatases Ppn1 and Ppn2 did not lead to increased polyP accumulation in steady state. This suggests that polyP levels of the cell are mainly controlled through synthesis and not through degradation. This interpretation is in line with our earlier findings showing that hyper-activation of the VTC complex by point mutations or overexpression of the regulatory subunit leads to higher polyP levels *in vivo* (Desfougères et al., 2016a) and that the polyP content of vacuoles may be sensed and communicated to the cytosol (Desfougères et al., 2016b). Studies on the mobilization of this store have so far been hampered by the fact that polyP turnover could be inhibited only partially because only a single vacuolar polyphosphatase was known. The identification of Ppn2 now allows experimenters to stabilize the vacuolar polyP pool, even under P<sub>i</sub> starvation conditions, where new polyP cannot be made. This suggests that Ppn1 and Ppn2 are the major players in the polyP mobilization required for growth. The discovery of the second vacuolar polyphosphatase thus opens the way for addressing the regulation of the vacuolar phosphate pool and for us to explore its impact on phosphate and energy homeostasis of the cell.

Accumulation of large polyP amounts as a P<sub>i</sub> reserve is a feature that is conserved in free-living microorganisms. In higher multicellular organisms, polyP assumes regulatory and signaling functions and may participate in bone mineralization (Müller et al., 2015). Discovering and studying functions of polyP that are unrelated to storage in yeast is complicated because of the extreme abundance of the vacuolar polyP pool (Gerasimaite et al., 2014; Indge, 1968; Urech et al., 1978), which can mask polyP dynamics in other cellular compartments. Selectively making this polyP pool

polyP of different chain length activates blood clotting by different mechanisms and displays different activities in pro-inflammatory signaling (Dinarvand et al., 2014; Smith et al., 2010).

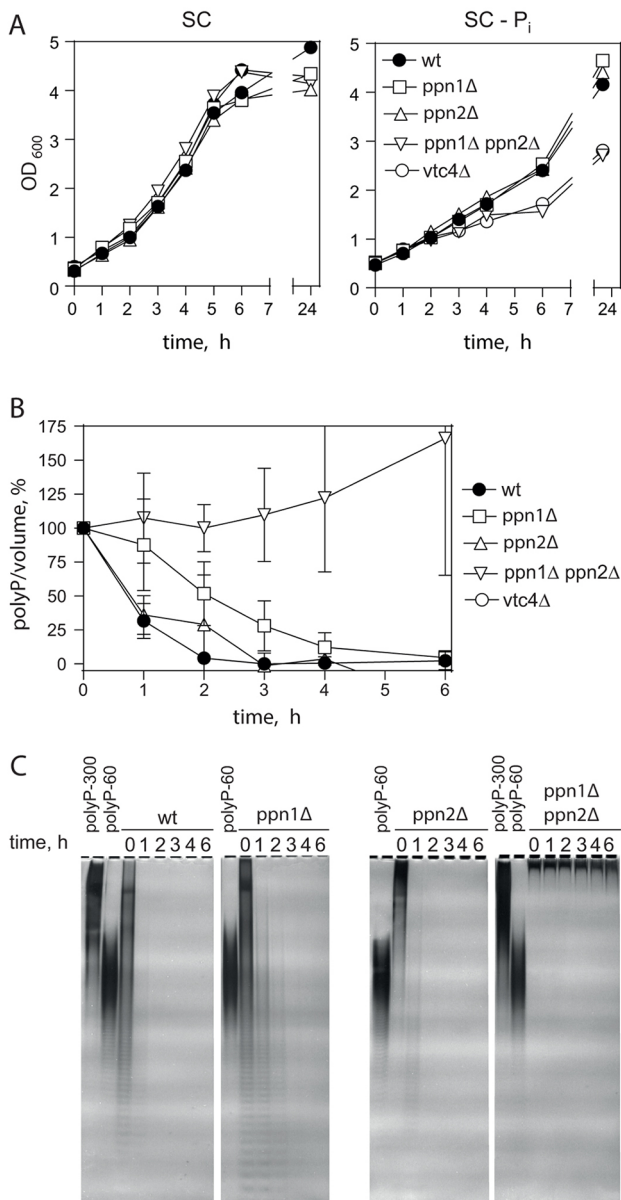


**Fig. 6. Vacuolar polyphosphatases in the mobilization of polyP stores under  $P_i$  starvation.** (A) Cell growth in SC and SC- $P_i$  medium. The cells were grown at 30°C overnight in SC medium to an  $OD_{600}$  of 0.5–2 and then inoculated in fresh medium at  $OD_{600}$  of 0.5. To monitor growth in SC- $P_i$ , the logarithmically growing precultures were washed with SC- $P_i$  once and resuspended in SC- $P_i$  at  $OD_{600}$ =0.5. The experiments were repeated three times and a representative experiment is shown. (B) PolyP mobilization upon  $P_i$  limitation. Logarithmically growing strains in SC were washed and transferred into SC- $P_i$ , and at the indicated time points polyP was isolated and quantified. The 0 h time point of each strain was used as the 100% reference. The data show polyP/ml of cell culture. Note that cells keep dividing (see A) but cannot synthesize new polyP on SC- $P_i$ , which dilutes their polyP stores per cell. Therefore, polyP content per culture volume represents the fate of the polyP stores brought into the culture at t=0 h. The experiment was repeated three times, mean±s.d. is shown. (C) Changes in polyP chain length in response to  $P_i$  availability. An amount equivalent to 0.2  $OD_{600}$  cells from B was treated with RNase A and proteinase K and analyzed on a 25% polyacrylamide gel.

inert by use of *ppn1Δ ppn2Δ* mutations could help experimenters to study polyP functions in other compartments, such as polyphosphorylation of nuclear proteins (Azevedo et al., 2015).

Protein polyphosphorylation requires an active VTC complex. However, it is unknown whether the polyP that is used for polyphosphorylation of nuclear proteins originates from the vacuolar pool. VTC is also found in the cell periphery, likely the endoplasmic reticulum, which is continuous with the nuclear membrane. It is not inconceivable that VTC might hand over polyP chains directly to cytosolic or nuclear proteins that use them for protein polyphosphorylation. The possibility of immobilizing the vacuolar polyP pool by the elimination of Ppn1 and Ppn2 may allow us to address such questions. It will also be instrumental in searching for and identifying potential additional polyphosphatases (Lichko et al., 2003).

## MATERIALS AND METHODS

### Materials

Creatine kinase, creatine phosphate and ATP were from Roche. PolyP-60 and polyP-300 were kind gifts from Toshikazu Shiba, Regenstiss Inc., Japan. Recombinant scPpx1 was purified as previously described (Gerasimaite et al., 2014). The concentration of polyP is reported as the concentration of  $P_i$  units. It was determined by degrading polyP with recombinant scPpx1 and measuring the released  $P_i$  with a Malachite Green assay (Hothorn et al., 2009).

Anti-HA monoclonal antibody HA.11 clone 16B12 (mouse ascites) (Covance, # MMS-101R) was used for immunoprecipitations. Anti-HA polyclonal antibody from rabbit (Abcam ab137838) was used at 1:2000 for western blotting. Anti-GFP (Torrey Pines Biolabs TP401), affinity purified from rabbit antisera, was used at 1:5000 for western blotting. Polyclonal antibodies to Pho8 and Vam3 were raised in rabbits using proteins expressed in *E. coli* as described (Müller et al., 2002; Pieren et al., 2010). The unpurified sera was used for western blotting at dilutions of 1:10,000. The secondary antibodies conjugated to IRDye 800 were from LiCor. Specificity of all antibodies had been verified by blotting of vacuoles from knockout strains or from strains expressing non-tagged proteins, respectively.

### Yeast strains and plasmids

Strains are listed in Table S1. Genes were deleted by replacing a complete ORF with a marker cassette (Janke et al., 2004; see Table S2 for PCR primers). Integration of the cassette into the correct region was confirmed by colony PCR, with one of the primers complementary to the promoter of the target gene and another primer complementary to the marker gene on the cassette. pRSx0x series plasmids were used as templates for amplifying cassettes with auxotrophic markers. *PEP4* and *PHO8* genes were deleted using plasmids pTS15 and pGP10, respectively (a kind gift from Tom Stevens, Eugene, OR). BY4742 *ppx1Δ ppn1Δ* was constructed from BY4742 *ppn1Δ::kanMX* (Euroscarf, acc.no. Y14286). BY4742 *vtc4Δ ppn1Δ* was constructed from BY4742 *vtc4Δ* (Euroscarf, Acc.no. Y16780).

To construct plasmids pRS415- $P_{GPD}$ -PPN2 and pRS415- $P_{GPD}$ -3HA-PPN2, yeast genomic DNA was isolated from strains BY4742  $P_{GPD}$ -PPN2 and BY4742  $P_{GPD}$ -3HA-Ppn2 as described previously (Breitkreutz et al., 2010) and the target genes were amplified using primer pairs RG077+RG074 and RG076+RG074, respectively. The resulting fragments were cloned into the pRS415GPD vector using BamHI and HindIII, or SpeI and HindIII restriction sites. The point mutations D68N and D98N were introduced by the QuikChange mutagenesis procedure using primers RG078+RG079 and RG080 and RG081, respectively.

### Cell growth and polyP isolation

Cell growth was assessed by measuring the optical density at 600 nm ( $OD_{600nm}$ ). To investigate polyP accumulation, growth in low- $P_i$  medium and degradation of polyP under phosphate starvation, precultures were grown in SC medium at 30°C for 24 h. From these, fresh cultures were inoculated and grown overnight at 30°C to reach an  $OD_{600nm}$  of 1–2. Then, the cells were sedimented (2 min, 3000 g), washed once with low phosphate medium (SC- $P_i$ ) and incubated at 30°C for 6 h. At the indicated time-points, 2.5  $OD_{600nm}$  units of cells were collected for polyP isolation.

To investigate growth in SC medium and the length of polyP chains at different growth phases, precultures were grown in SC for 48 h at 30°C. Then, the cells were diluted to an OD<sub>600nm</sub> of ~0.1 with fresh medium and further incubated at 30°C. The following samples were collected and processed immediately: lag phase (at OD<sub>600nm</sub> of ~0.1, 3 h incubation), early exponential phase (at OD<sub>600nm</sub> of ~0.4–0.6, 6–7 h incubation), stationary phase (at OD<sub>600nm</sub> of 3–4, 24 h incubation). PolyP was isolated from 2–2.5 OD<sub>600nm</sub> units of cells by phenol/chloroform and glass bead extraction as described previously (Lonetti et al., 2011) and dissolved in 100 µl TE buffer (10 mM Tris-HCl pH 7.4, 0.5 mM EDTA). Isolated polyP was quantified by enzymatic hydrolysis with an excess of recombinant scPpx1: ~50 nmol of isolated polyP was incubated in 100 µl of 5 mM Tris-HCl pH 7.0, 1.5 mM MgCl<sub>2</sub> and 0.4 µg/ml scPpx1 at 37°C for 1.5–2 h. An aliquot of 10 µl was mixed with 90 µl water and phosphate was quantified by adding 150 µl Malachite Green reagent (86 µl 28 mM ammonium heptamolybdate in 12.5% H<sub>2</sub>SO<sub>4</sub> and 64 µl 0.76 mM malachite green in 0.35% polyvinyl alcohol) and measuring absorbance at 595 nm.

### Vacuole isolation

For vacuole isolation, the cells were grown in 1 l YPD medium at 30°C overnight to an OD<sub>600 nm</sub> of 0.8–1.9 and vacuoles were isolated by floatation in a stepwise Ficoll 400 gradient as described previously (Gerasimaite et al., 2014). Unless indicated otherwise, the fractionation solutions contained 0.5× protease inhibitor cocktail (PIC): 50 µM pefabloc SC, 50 ng/ml leupeptin, 25 µM O-phenanthroline and 250 ng/ml pepstatin A, and 1 mM PMSF. Vacuole concentration is expressed as concentration of total vacuolar protein as determined by a Bradford assay, using bovine serum albumin (BSA) as a standard.

### Microscopy

The cells were grown in SC medium overnight to an OD<sub>600 nm</sub> of 1–2. For staining the vacuole membrane, 0.2 OD<sub>600 nm</sub> units of cells were resuspended in 1 ml SC medium containing 10 µM FM4-64 and incubated at 30°C for 1 h. The cells were washed once with a fresh medium and chased for an additional hour. Cells were observed using a LEICA DMI6000 B inverted microscope with a 100×1.4 NA lens, connected to a Hamamatsu digital CCD camera (ORCA-R2 C10600-10B) and an X-Cite® series 120Q UV lamp. Appropriate filters were used to visualize GFP and FM4–64 fluorescence.

### Ppn2 topology

The orientation of Ppn2 relative to the vacuole membrane was probed by limited proteolysis of Ppn2 N- and C-terminal fusions with yeGFP. Isolated vacuoles were resuspended in PS buffer (10 mM PIPES-KOH pH 6.8, 200 mM sorbitol) to 0.02 mg/ml and mixed with an equal volume of proteinase K (20 µg/ml in PS buffer). The samples were incubated for 5 min on ice and proteins were precipitated with 10% trichloroacetic acid (TCA). Untreated controls received either no proteinase K at 0 min or proteinase K was added after TCA. The samples were fractionated on SDS-PAGE gels and yeGFP was detected by western blotting.

### Immunoprecipitation of HA–Ppn2

All solutions contained 1×PIC and 1 mM PMSF. 200 µg vacuoles in 200–400 µl were mixed with 1 ml PS buffer, collected by centrifugation (7000 g, 10 min, 4°C) and gently resuspended in 360 µl solubilization buffer (20 mM PIPES-KOH pH 6.8, 150 mM KCl). 40 µl 5% Triton X-100 was added, the samples were shaken vigorously at 4°C for 20 min, centrifuged (15 min, 22,000 g at 4°C). 4 µl HA.11 clone 16B12 monoclonal antibody was added to the supernatant together with 30 µl protein-G-agarose beads (Roche) equilibrated in the solubilization buffer. The samples were incubated on a rotating wheel (8°C, 2 h), then the beads were washed once with solubilization buffer with Triton X-100 and three times with solubilization buffer, and were then resuspended in 180 µl of solubilization buffer. 1.5 µl of the resulting suspension was used for an 80 µl reaction (single time-point). This corresponds to 1.5 µg of starting vacuole material. The immunoprecipitation efficiency varied between 12 and 35% of the total input in different experiments.

### Polyphosphatase activity assays

Polyphosphatase activity of immunoprecipitated 3HA–Ppn2 was assayed in a buffer containing 20 mM PIPES-KOH pH 6.8, 150 mM KCl, 1 mM ZnCl<sub>2</sub> and 30 µM polyP-60. The reactions were started by adding 3HA–Ppn2 adsorbed onto beads (1.5 µl beads in 80 µl) and incubated at 27°C with vigorous shaking. At the indicated time points, 80 µl aliquots were withdrawn and the reaction was stopped by mixing with 160 µl of stop buffer (10 mM PIPES-KOH pH 6.8, 150 mM KCl, 15 µM DAPI, 12 mM EDTA). PolyP was detected by measuring the characteristic DAPI-polyP fluorescence (excitation at 415 nm, emission at 550 nm, 530 nm cut-off) in a black 96-well plate.

When P<sub>i</sub> release was monitored, the reactions were performed in 150 µl volume of the same buffer in the presence of 15 µl beads. The reactions were incubated at 27°C for 30 min, then 100 µl aliquots were withdrawn and mixed with 10 µl 1 M H<sub>2</sub>SO<sub>4</sub>. In parallel, the same quantity of polyP-60 was hydrolyzed with 1 M HClO<sub>4</sub> (30 min, 99°C). Released P<sub>i</sub> was detected by adding 150 µl Malachite Green reagent and measuring absorbance at 595 nm.

For measuring polyphosphatase activities of vacuole lysates, vacuoles were isolated without PIC. The reactions were started by adding vacuoles (final concentration 0.002 mg/ml) to a buffer containing 20 mM PIPES-KOH pH 6.8, 150 mM KCl, 1 mM ZnCl<sub>2</sub> or MgCl<sub>2</sub>, 0.1% Triton X-100, 1×PIC and 1 mM PMSF. After different periods of incubation at 27°C, 80 µl aliquots were withdrawn, the reactions were stopped and the remaining polyP was detected as described above. Values for the 0 min time-point represent reactions that had been performed with heat-inactivated (10 min, 99°C) vacuoles.

### Covalent modification of polyP-60 ends

Terminal phosphate groups of polyP chains were blocked by attaching spermidine via a phosphoamidate linkage as described (Choi et al., 2010). Briefly, 5 mM polyP-60 or polyP-300 were incubated in 100 µl of 100 mM MES-NaOH pH 6.5 in the presence of 300 mM N-(3-dimethylaminopropyl)-N'-ethylcarbodiimide hydrochloride (EDAC) and 70 mM spermidine-HCl at 37°C overnight. In the control reaction, EDAC was omitted. At the end of the reaction, LiCl was added to give a 1 M final concentration and unreacted spermidine-HCl and EDAC were removed by gel filtration on a sephadex G-25 column equilibrated with 1 M LiCl. PolyP was precipitated with 500 µl acetone, centrifuged (22,000 g, 30 min), washed once with acetone, air-dried and dissolved in water. The concentration was estimated by DAPI fluorescence using unmodified polyP-60 as a standard. 30 µM of chemically modified and control polyP was used in the reaction with immunoprecipitated 3HA–Ppn2.

### Acknowledgements

We thank Toshikazu Shiba (Regenetiss Inc., Japan) for synthetic polyP-60 and polyP-300. We are grateful to Andrea Schmidt, Lydie Michailat-Mayer and Yann Desfougères for yeast strains and discussions.

### Competing interests

The authors declare no competing or financial interests.

### Author contributions

A.M. conceived the project. R.G. designed and performed the experiments, R.G. and A.M. analyzed the results and wrote the manuscript.

### Funding

This work was supported by the European Research Council (233458) and Schweizerischer Nationalfonds zur Förderung der Wissenschaftlichen Forschung (SNF) (144258 and 163477/1) (to A.M.).

### Supplementary information

Supplementary information available online at <http://jcs.biologists.org/lookup/doi/10.1242/jcs.201061.supplemental>

### References

- Andreeva, N., Trilisenko, L., Eldarov, M. and Kulakovskaya, T. (2015). Polyphosphatase PPN1 of *Saccharomyces cerevisiae*: switching of exopolyphosphatase and endopolyphosphatase activities. *PLoS ONE* **10**, e0119594.
- Andreini, C., Bertini, I., Cavallaro, G., Holliday, G. L. and Thornton, J. M. (2008). Metal ions in biological catalysis: from enzyme databases to general principles. *J. Biol. Inorganic Chem.* **13**, 1205–1218.

- Azevedo, C., Livermore, T. and Saiardi, A.** (2015). Protein polyphosphorylation of lysine residues by inorganic polyphosphate. *Mol. Cell* **58**, 71-82.
- Babst, M., Sato, T. K., Banta, L. M. and Emr, S. D.** (1997). Endosomal transport function in yeast requires a novel AAA-type ATPase, Vps4p. *EMBO J.* **16**, 1820-1831.
- Biasini, M., Bienert, S., Waterhouse, A., Arnold, K., Studer, G., Schmidt, T., Kiefer, F., Cassarino, T. G., Bertoni, M., Bordoli, L. et al.** (2014). SWISS-MODEL: modelling protein tertiary and quaternary structure using evolutionary information. *Nucleic Acids Res.* **42**, W252-W258.
- Brachmann, C. B., Davies, A., Cost, G. J., Caputo, E., Li, J., Hieter, P. and Boeke, J. D.** (1998). Designer deletion strains derived from *Saccharomyces cerevisiae* S288C: a useful set of strains and plasmids for PCR-mediated gene disruption and other applications. *Yeast* **14**, 115-132.
- Breitkreutz, A., Choi, H., Sharom, J. R., Boucher, L., Neduva, V., Larsen, B., Lin, Z. Y., Breitkreutz, B. J., Stark, C., Liu, G. et al.** (2010). A global protein kinase and phosphatase interaction network in yeast. *Science* **328**, 1043-1046.
- Bru, S., Martínez-Láinez, J. M., Hernández-Ortega, S., Quandt, E., Torres-Torronteras, J., Martí, R., Canadell, D., Ariño, J., Sharma, S., Jiménez, J. et al.** (2016). Polyphosphate is involved in cell cycle progression and genomic stability in *Saccharomyces cerevisiae*. *Mol. Microbiol.* **101**, 367-380.
- Cartwright, J. L. and McLennan, A. G.** (1999). The *Saccharomyces cerevisiae* YOR163w gene encodes a diadenosine 5', 5''-P<sub>1</sub>,P<sub>6</sub>-hexaphosphate (Ap<sub>6</sub>A) hydrolase member of the MutT motif (Nudix hydrolase) family. *J. Biol. Chem.* **274**, 8604-8610.
- Choi, S. H., Collins, J. N. R., Smith, S. A., Davis-Harrison, R. L., Rienstra, C. M. and Morrissey, J. H.** (2010). Phosphoramidate end labeling of inorganic polyphosphates: facile manipulation of polyphosphate for investigating and modulating its biological activities. *Biochemistry* **49**, 9935-9941.
- Cini, N. and Ball, V.** (2014). Polyphosphates as inorganic polyelectrolytes interacting with oppositely charged ions, polymers and deposited on surfaces: fundamentals and applications. *Adv. Colloid Interface Sci.* **209**, 84-97.
- Cremers, C. M., Knoefler, D., Gates, S., Martin, N., Dahl, J.-U., Lempart, J., Xie, L., Chapman, M. R., Galvan, V., Southworth, D. R. et al.** (2016). Polyphosphate: a conserved modifier of amyloidogenic processes. *Mol. Cell* **63**, 768-780.
- Dahl, J.-U., Gray, M. J. and Jakob, U.** (2015). Protein quality control under oxidative stress conditions. *J. Mol. Biol.* **427**, 1549-1563.
- Desfougères, Y., Gerasimaitė, R. U., Jessen, H. J. and Mayer, A.** (2016a). Vtc5, a novel subunit of the vacuolar transporter chaperone complex, regulates polyphosphate synthesis and phosphate homeostasis in yeast. *J. Biol. Chem.* **291**, 22262-22275.
- Desfougères, Y., Neumann, H. and Mayer, A.** (2016b). Organelle size control - increasing vacuole content activates SNAREs to augment organelle volume through homotypic fusion. *J. Cell Sci.* **129**, 2817-2828.
- Dinarvand, P., Hassanian, S. M., Qureshi, S. H., Manithody, C., Eissenberg, J. C., Yang, L. and Rezaie, A. R.** (2014). Polyphosphate amplifies proinflammatory responses of nuclear proteins through interaction with receptor for advanced glycation end products and P2Y<sub>1</sub> purinergic receptor. *Blood* **123**, 935-945.
- Docampo, R. and Huang, G.** (2016). Acidocalcisomes of eukaryotes. *Curr. Opin. Cell Biol.* **41**, 66-72.
- Docampo, R., de Souza, W., Miranda, K., Rohloff, P. and Moreno, S. N. J.** (2005). Acidocalcisomes - conserved from bacteria to man. *Nat. Rev. Microbiol.* **3**, 251-261.
- Eiser, J. J.** (2012). Phosphorus: a limiting nutrient for humanity? *Curr. Opin. Biotechnol.* **23**, 833-838.
- Faxalv, L., Boknas, N., Strom, J. O., Tengvall, P., Theodorsson, E., Ramstrom, S. and Lindahl, T. L.** (2013). Putting polyphosphates to the test: evidence against platelet-induced activation of factor XII. *Blood* **122**, 3818-3824.
- Fernandez, M. P., Gascon, S. and Schwencke, J.** (1981). Some enzymatic properties of vacuolar alkaline phosphatase from yeast. *Curr. Microbiol.* **6**, 121-126.
- Galizzi, M., Bustamante, J. M., Fang, J., Miranda, K., Soares Medeiros, L. C., Tarleton, R. L. and Docampo, R.** (2013). Evidence for the role of vacuolar soluble pyrophosphatase and inorganic polyphosphate in *Trypanosoma cruzi* persistence. *Mol. Microbiol.* **90**, 699-715.
- Gerasimaitė, R., Sharma, S., Desfougères, Y., Schmidt, A. and Mayer, A.** (2014). Coupled synthesis and translocation restrains polyphosphate to acidocalcisome-like vacuoles and prevents its toxicity. *J. Cell Sci.* **127**, 5093-5104.
- Gray, M. J., Wholey, W.-Y., Wagner, N. O., Cremers, C. M., Mueller-Schickert, A., Hock, N. T., Krieger, A. G., Smith, E. M., Bender, R. A., Bardwell, J. C. A. et al.** (2014). Polyphosphate is a primordial chaperone. *Mol. Cell* **53**, 689-699.
- Harold, F. M.** (1966). Inorganic polyphosphates in biology: structure, metabolism, and function. *Bacteriol. Rev.* **30**, 772-794.
- Hothorn, M., Neumann, H., Lenherr, E. D., Wehner, M., Rybin, V., Hassa, P. O., Uttenweiler, A., Reinhardt, M., Schmidt, A., Seiler, J. et al.** (2009). Catalytic core of a membrane-associated eukaryotic polyphosphate polymerase. *Science* **324**, 513-516.
- Huh, W.-K., Falvo, J. V., Gerke, L. C., Carroll, A. S., Howson, R. W., Weissman, J. S. and O'Shea, E. K.** (2003). Global analysis of protein localization in budding yeast. *Nature* **425**, 686-691.
- Hurley, J. H. and Emr, S. D.** (2006). The ESCRT complexes: structure and mechanism of a membrane-trafficking network. *Annu. Rev. Biophys. Biomol. Struct.* **35**, 277-298.
- Indge, K. J.** (1968). Polyphosphates of the yeast cell vacuole. *J. Gen. Microbiol.* **51**, 447-455.
- Janke, C., Magiera, M. M., Rathfelder, N., Taxis, C., Reber, S., Maekawa, H., Moreno-Borchart, A., Doenges, G., Schwob, E., Schiebel, E. et al.** (2004). A versatile toolbox for PCR-based tagging of yeast genes: new fluorescent proteins, mouse markers and promoter substitution cassettes. *Yeast* **21**, 947-962.
- Jones, E. W., Zubenko, G. S. and Parker, R. R.** (1982). PEP4 gene function is required for expression of several vacuolar hydrolases in *Saccharomyces cerevisiae*. *Genetics* **102**, 665-677.
- Keasling, J. D.** (1997). Regulation of intracellular toxic metals and other cations by hydrolysis of polyphosphate. *Ann. N. Y. Acad. Sci.* **829**, 242-249.
- Kim, K.-S., Rao, N. N., Fraley, C. D. and Kornberg, A.** (2002). Inorganic polyphosphate is essential for long-term survival and virulence factors in *Shigella* and *Salmonella* spp. *Proc. Natl. Acad. Sci. USA* **99**, 7675-7680.
- Kizawa, K., Aono, T. and Ohtomo, R.** (2016). PHO8 gene coding alkaline phosphatase of *Saccharomyces cerevisiae* is involved in polyphosphate metabolism. *J. Gen. Appl. Microbiol.* **62**, 297-302.
- Kornberg, A., Rao, N. N. and Ault-Riché, D.** (1999). Inorganic polyphosphate: a molecule of many functions. *Annu. Rev. Biochem.* **68**, 89-125.
- Kumble, K. D. and Kornberg, A.** (1995). Inorganic polyphosphate in mammalian cells and tissues. *J. Biol. Chem.* **270**, 5818-5822.
- Lander, N., Ulrich, P. N. and Docampo, R.** (2013). Trypanosoma brucei vacuolar transporter chaperone 4 (TbVtc4) is an acidocalcisome polyphosphate kinase required for in vivo infection. *J. Biol. Chem.* **288**, 34205-34216.
- Lee, A. and Whitesides, G. M.** (2010). Analysis of inorganic polyphosphates by capillary gel electrophoresis. *Anal. Chem.* **82**, 6838-6846.
- Li, S. C. and Kane, P. M.** (2009). The yeast lysosome-like vacuole: endpoint and crossroads. *Biochim. Biophys. Acta* **1793**, 650-663.
- Lichko, L. P., Kulakovskaya, T. V. and Kulaev, I. S.** (2000). Purification and characterization of a soluble polyphosphatase from mitochondria of *Saccharomyces cerevisiae*. *Biochemistry* **65**, 355-360.
- Lichko, L. P., Andreeva, N. A., Kulakovskaya, T. V. and Kulaev, I. S.** (2003). Exopolyphosphatases of the yeast *Saccharomyces cerevisiae*. *FEMS Yeast Res.* **3**, 233-238.
- Lichko, L., Kulakovskaya, T., Pestov, N. and Kulaev, I.** (2006). Inorganic polyphosphates and exopolyphosphatases in cell compartments of the yeast *Saccharomyces cerevisiae* under inactivation of PPX1 and PPN1 genes. *Biosci. Rep.* **26**, 45-54.
- Lichko, L. P., Kulakovskaya, T. V., Kulakovskaya, E. V. and Kulaev, I. S.** (2008). Inactivation of PPX1 and PPN1 genes encoding exopolyphosphatases of *Saccharomyces cerevisiae* does not prevent utilization of polyphosphates as phosphate reserve. *Biochemistry* **73**, 985-989.
- Livermore, T. M., Chubb, J. R. and Saiardi, A.** (2016). Developmental accumulation of inorganic polyphosphate affects germination and energetic metabolism in *Dictyostelium discoideum*. *Proc. Natl. Acad. Sci. USA* **113**, 996-1001.
- Lonetti, A., Szigyarto, Z., Bosch, D., Loss, O., Azevedo, C. and Saiardi, A.** (2011). Identification of an evolutionarily conserved family of inorganic polyphosphate endopolyphosphatases. *J. Biol. Chem.* **286**, 31966-31974.
- Lusby, E. W., Jr and McLaughlin, C. S.** (1980). The metabolic properties of acid soluble polyphosphates in *Saccharomyces cerevisiae*. *Mol. Gen. Genet.* **178**, 69-76.
- Mohamed, M. F. and Hoffelder, F.** (2013). Efficient, crosswise catalytic promiscuity among enzymes that catalyze phosphoryl transfer. *Biochim. Biophys. Acta* **1834**, 417-424.
- Morrissey, J. H. and Smith, S. A.** (2015). Polyphosphate as modulator of hemostasis, thrombosis, and inflammation. *J. Thromb. Haemostas.* **13** Suppl. 1, S92-S97.
- Müller, O., Bayer, M. J., Peters, C., Andersen, J. S., Mann, M. and Mayer, A.** (2002). The Vtc proteins in vacuole fusion: coupling NSF activity to V(0) trans-complex formation. *EMBO J.* **21**, 259-269.
- Müller, F., Mutch, N. J., Schenk, W. A., Smith, S. A., Esterl, L., Spronk, H. M., Schmidbauer, S., Gahl, W. A., Morrissey, J. H. and Renné, T.** (2009). Platelet polyphosphates are proinflammatory and procoagulant mediators in vivo. *Cell* **139**, 1143-1156.
- Müller, W. E. G., Tolba, E., Schröder, H. C. and Wang, X.** (2015). Polyphosphate: a morphogenetically active implant material serving as metabolic fuel for bone regeneration. *Macromol. Biosci.* **15**, 1182-1197.
- Nocek, B., Kochinyan, S., Proudfoot, M., Brown, G., Evdokimova, E., Osipiuk, J., Edwards, A. M., Savchenko, A., Joachimiak, A. and Yakinun, A. F.** (2008). Polyphosphate-dependent synthesis of ATP and ADP by the family-2 polyphosphate kinases in bacteria. *Proc. Natl. Acad. Sci. USA* **105**, 17730-17735.
- Odorizzi, G., Babst, M. and Emr, S. D.** (1998). Fab1p PtdIns(3)P 5-kinase function essential for protein sorting in the multivesicular body. *Cell* **95**, 847-858.
- Ogawa, N., DeRisi, J. and Brown, P. O.** (2000). New components of a system for phosphate accumulation and polyphosphate metabolism in *Saccharomyces*

- cerevisiae revealed by genomic expression analysis. *Mol. Biol. Cell* **11**, 4309-4321.
- Pick, U. and Weiss, M.** (1991). Polyphosphate hydrolysis within acidic vacuoles in response to amine-induced alkaline stress in the Halotolerant Alga *Dunaliella salina*. *Plant Physiol.* **97**, 1234-1240.
- Pieren, M., Schmidt, A. and Mayer, A.** (2010). The SM protein Vps33 and the t-SNARE H(abc) domain promote fusion pore opening. *Nat. Struct. Mol. Biol.* **17**, 710-717.
- Rao, N. N., Gómez-García, M. R. and Kornberg, A.** (2009). Inorganic polyphosphate: essential for growth and survival. *Annu. Rev. Biochem.* **78**, 605-647.
- Reggiori, F. and Pelham, H. R. B.** (2001). Sorting of proteins into multivesicular bodies: ubiquitin-dependent and -independent targeting. *EMBO J.* **20**, 5176-5186.
- Reynolds, S. M., Käll, L., Riffle, M. E., Bilmes, J. A. and Noble, W. S.** (2008). Transmembrane topology and signal peptide prediction using dynamic bayesian networks. *PLoS Comput. Biol.* **4**, e1000213.
- Rohloff, P. and Docampo, R.** (2008). A contractile vacuole complex is involved in osmoregulation in *Trypanosoma cruzi*. *Exp. Parasitol.* **118**, 17-24.
- Ruiz, F. A., Rodrigues, C. O. and Docampo, R.** (2001). Rapid changes in polyphosphate content within acidocalcisomes in response to cell growth, differentiation, and environmental stress in *Trypanosoma cruzi*. *J. Biol. Chem.* **276**, 26114-26121.
- Safrany, S. T., Ingram, S. W., Cartwright, J. L., Falck, J. R., McLennan, A. G., Barnes, L. D. and Shears, S. B.** (1999). The diadenosine hexaphosphate hydrolases from *Schizosaccharomyces pombe* and *Saccharomyces cerevisiae* are homologues of the human diphosphoinositol polyphosphate phosphohydrolase. Overlapping substrate specificities in a MutT-type protein. *J. Biol. Chem.* **274**, 21735-21740.
- Sethuraman, A., Rao, N. N. and Kornberg, A.** (2001). The endopolyphosphatase gene: essential in *Saccharomyces cerevisiae*. *Proc. Natl. Acad. Sci. USA* **98**, 8542-8547.
- Shi, X. and Kornberg, A.** (2005). Endopolyphosphatase in *Saccharomyces cerevisiae* undergoes post-translational activations to produce short-chain polyphosphates. *FEBS Lett.* **579**, 2014-2018.
- Simm, C., Lahner, B., Salt, D., LeFurgey, A., Ingram, P., Yandell, B. and Eide, D. J.** (2007). *Saccharomyces cerevisiae* vacuole in zinc storage and intracellular zinc distribution. *Eukaryot. Cell* **6**, 1166-1177.
- Smith, S. A., Choi, S. H., Davis-Harrison, R., Huyck, J., Boettcher, J., Rienstra, C. M. and Morrissey, J. H.** (2010). Polyphosphate exerts differential effects on blood clotting, depending on polymer size. *Blood* **116**, 4353-4359.
- Stotz, S. C., Scott, L. O. M., Drummond-Main, C., Avchalumov, Y., Giroto, F., Davidsen, J., Gómez-García, M. R., Rho, J. M., Pavlov, E. V. and Colicos, M. A.** (2014). Inorganic polyphosphate regulates neuronal excitability through modulation of voltage-gated channels. *Mol. Brain* **7**, 42.
- Thomas, M. R. and O'Shea, E. K.** (2005). An intracellular phosphate buffer filters transient fluctuations in extracellular phosphate levels. *Proc. Natl. Acad. Sci. USA* **102**, 9565-9570.
- Trilisenko, L. V., Andreeva, N. A., Eldarov, M. A., Dumina, M. V. and Kulakovskaya, T. V.** (2015). Polyphosphates and polyphosphatase activity in the yeast *Saccharomyces cerevisiae* during overexpression of the DDP1 gene. *Biochemistry* **80**, 1312-1317.
- Urech, K., Durr, M., Boller, T., Wiemken, A. and Schwencke, J.** (1978). Localization of polyphosphate in vacuoles of *Saccharomyces cerevisiae*. *Arch. Microbiol.* **116**, 275-278.
- Uttenweiler, A., Schwarz, H., Neumann, H. and Mayer, A.** (2007). The vacuolar transporter chaperone (VTC) complex is required for microautophagy. *Mol. Biol. Cell* **18**, 166-175.
- Vardi, N., Levy, S., Assaf, M., Carmi, M. and Barkai, N.** (2013). Budding yeast escape commitment to the phosphate starvation program using gene expression noise. *Curr. Biol.* **23**, 2051-2057.
- Wang, Q.-H., Hu, W.-X., Gao, W. and Bi, R.-C.** (2006). Crystal structure of the diadenosine tetraphosphate hydrolase from *Shigella flexneri* 2a. *Proteins* **65**, 1032-1035.
- Wild, R., Gerasimaite, R., Jung, J.-Y., Truffault, V., Pavlovic, I., Schmidt, A., Saiardi, A., Jessen, H. J., Poirier, Y., Hothorn, M. et al.** (2016). Control of eukaryotic phosphate homeostasis by inositol polyphosphate sensor domains. *Science* **352**, 986-990.
- Wurst, H. and Kornberg, A.** (1994). A soluble exopolyphosphatase of *Saccharomyces cerevisiae*. Purification and characterization. *J. Biol. Chem.* **269**, 10996-11001.
- Wurst, H., Shiba, T. and Kornberg, A.** (1995). The gene for a major exopolyphosphatase of *Saccharomyces cerevisiae*. *J. Bacteriol.* **177**, 898-906.
- Zhuo, S., Clemens, J. C., Stone, R. L. and Dixon, J. E.** (1994). Mutational analysis of a Ser/Thr phosphatase. Identification of residues important in phosphoesterase substrate binding and catalysis. *J. Biol. Chem.* **269**, 26234-26238.